AD-A085 201 HARRY DIAMOND LABS ADELPHI MD F/G 17/6
USE OF A PARALLEL PLATE TRANSMISSION LINE TO CALIBRATE A FIBER---ETC(U)
JAN 80 A A CUNEO, J L LOFTUS
UNCLASSIFIED HDL-TM-80-11 NL

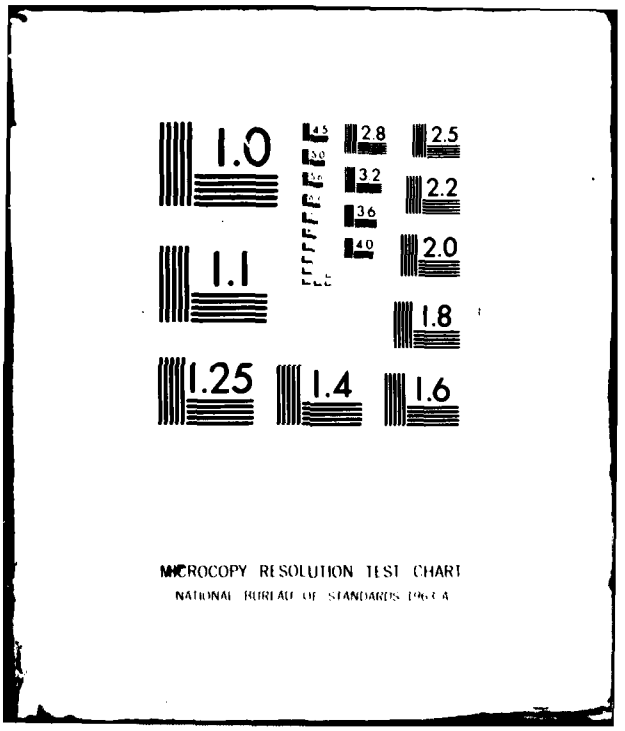
1.0
1.1
1.25
1.4
1.6
2.8
3.2
3.6
4.0
2.5
2.2
2.0
1.8
MICROCOPY RESOLUTION TEST CHART
NATIONAL BUREAU OF STANDARDS 1963 A

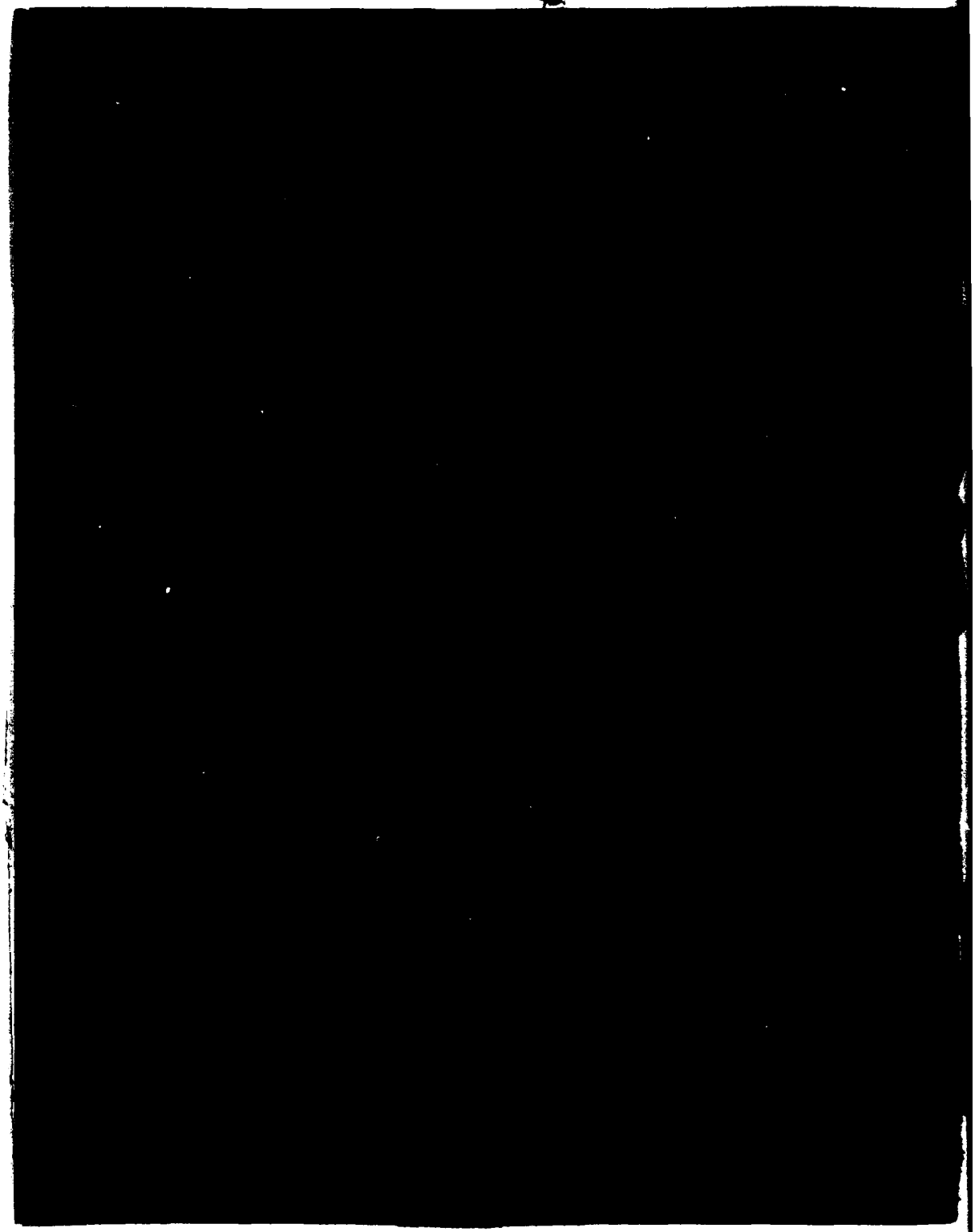

UNCLASSIFIED

SECURITY CLASSIFICATION OF THIS PAGE (When Data Entered)

REPORT DOCUMENTATION PAGE	READ INSTRUCTIONS BEFORE COMPLETING FORM
1. REPORT NUMBER: HDL-TM-80-11	2. GOVT ACCESSION NO.: AD-A085201
3. RECIPIENT'S CATALOG NUMBER	
4. TITLE (and Subtitle): Use of a Parallel Plate Transmission Line to Calibrate a Fiber-Optic Coupled Magnetic Field Sensor	5. TYPE OF REPORT & PERIOD COVERED: Technical Memorandum
6. PERFORMING ORG. REPORT NUMBER	
7. AUTHOR(s): Andrew A. Cuneo, Jr. James J. Loftus	8. CONTRACT OR GRANT NUMBER(s)
9. PERFORMING ORGANIZATION NAME AND ADDRESS: Harry Diamond Laboratories 2800 Powder Mill Road Adelphi, MD 20783	10. PROGRAM ELEMENT, PROJECT, TASK AREA & WORK UNIT NUMBERS: Program Ele: 6.21.20.A
11. CONTROLLING OFFICE NAME AND ADDRESS: US Army Materiel Development & Readiness Command Alexandria, VA 22333	12. REPORT DATE: January 1980 13. NUMBER OF PAGES: 16
14. MONITORING AGENCY NAME & ADDRESS(if different from Controlling Office)	15. SECURITY CLASS. (of this report): UNCLASSIFIED 15a. DECLASSIFICATION/DOWNGRADING SCHEDULE

16. DISTRIBUTION STATEMENT (of this Report)

Approved for public release; distribution unlimited.

17. DISTRIBUTION STATEMENT (of the abstract entered in Block 20, if different from Report)

DTIC ELECTE JUN 6 1980 S D

18. SUPPLEMENTARY NOTES

DRCMS Code: 612120.H250011
HDL Project: X759M4
DA Proj: 1L162120AH25

A

19. KEY WORDS (Continue on reverse side if necessary and identify by block number)

Magnetic field
Sensor
Fiber optic
Transmission line

20. ABSTRACT (Continue on reverse side if necessary and identify by block number)

It is vitally important to accurately measure the field components of a simulated electromagnetic pulse (EMP), to determine both the waveshape and the amplitude of the electromagnetic test environment. A parallel plate transmission line is used to calibrate a magnetic field sensor as well as to determine the field enhancement factor when the sensor is mounted on the compact transmitter of an optical electronic data-link system. The transmitter is coupled to the recording instrumentation by means of a fiber-optic → over

DD FORM 1 JAN 73 1473 EDITION OF 1 NOV 65 IS OBSOLETE

UNCLASSIFIED

SECURITY CLASSIFICATION OF THIS PAGE (When Data Entered)

163050

Abstract (Cont'd)

cable rather than an rf cable, thus eliminating a spurious signal pickup source. Some comments are also made on the use of enhancement factors for magnetic field sensors mounted on cubical boxes.

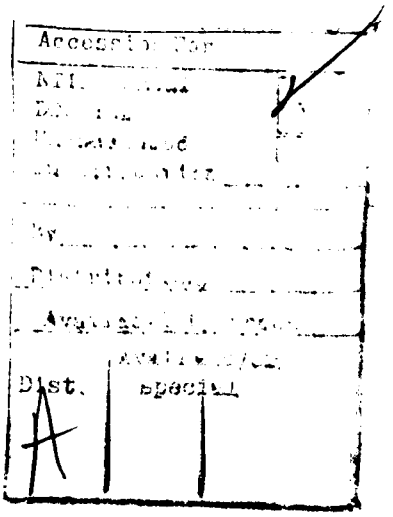

CONTENTS

FIGURES

1. INTRODUCTION

It is vitally important to accurately measure the field components of a simulated electromagnetic pulse (EMP), to determine both the waveshape and the amplitude of the electromagnetic test environment. Significant improvements in the techniques used to measure the field components have not been forthcoming in recent years.

In this report is discussed the use of a parallel plate transmission line to determine the calibration and response of the magnetic field sensors designed by the Stanford Research Institute (SRI). Also discussed is the field enhancement factor when the sensor is mounted on the compact transmitter of an optical electronic data-link system. The transmitter is coupled to the recording instrumentation by means of a fiber-optic cable rather than an rf cable, thus eliminating a spurious signal pickup source.

2. TRANSMISSION LINES

2.1 Physical Dimensions and Impedance

A transmission line (see fig. 1) was constructed at the Woodbridge Research Facility of Harry Diamond Laboratories (HDL). The line was 18 m long, tapered in width and height at both ends, with a working volume at the center of 2.0 m wide by 0.8 m high. The line was constructed so that the calculated impedance would be 102 ohms. Time-domain reflectometry measurements of the line showed the impedance to be approximately 90 ohms, and this value was used as the termination resistance. The transmission line was repetitively pulse driven by an HDL-built mercury reed pulser, discharging a 1 μs coaxial line which had been charged to 2 kV. The impedance mismatch at the drive point was minimized by the use of an unbalanced 50- to 90-ohm resistive pad. The pulse applied to this pad had a rise time of less than 0.2 ns (10 to 90%) and a peak level of 1 kV into 50 ohms.

2.2 Drive Voltage and Field Calculations

The current and the voltage at both the termination and input were observed and recorded and the voltage at the working volume, V_L, was found by measurement to be 370.0 V. The instrument used to record the data was a Tektronix 7904 mainframe oscilloscope with a 7A19 vertical amplifier and 7B92 time base. The electric field is calculated to be

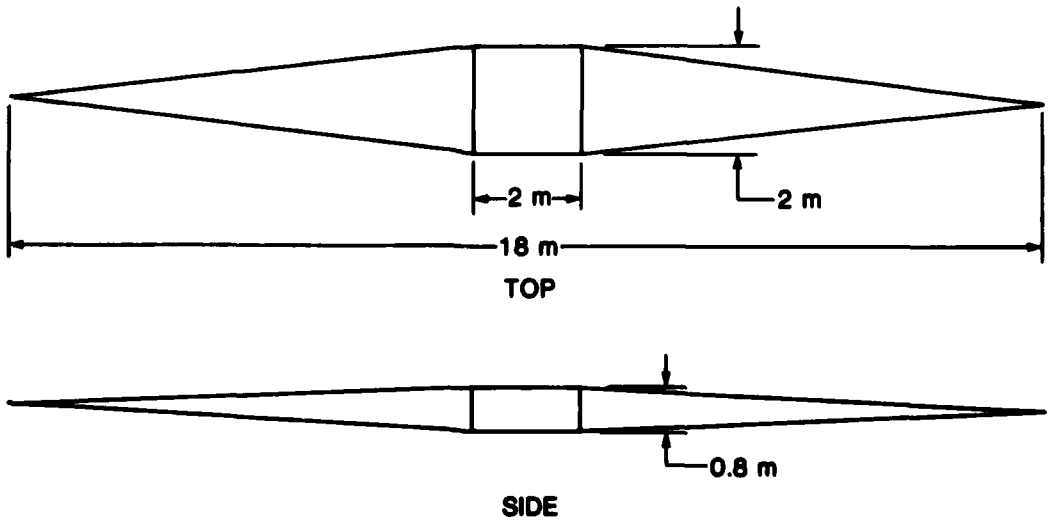

Figure 1. Parallel plate transmission line.

$$\frac{V_L}{h} = \frac{370.0\ V}{0.8\ m} = 463.0\ V/m\ ,$$

and the magnetic field is

$$H = \frac{463.0\ V/m}{120\ \pi\ ohms} = 1.23\ A/m\ .$$

2.3 Magnetic Field Measurements with B-Dot Sensor

The magnetic field within the transmission line was observed and recorded, using an EG&G B-dot sensor (MGL-2BR), balun (DLT96), and 1-μs integrator (RCI-1B). Using a derived calibration factor,[1] the measured field was found to be 1.19 A/m or 449.0 V/m. This value is 3 percent less than calculated. This measurement was made with the axis of the B-dot sensor 12.7 cm above the lower plate of the transmission line. A second measurement with the B-dot sensor elevated to 50.8 cm yielded an H-field value of 1.35 A/m, which is 10 percent higher than calculated. The H-field was observed and recorded as the B-dot position was varied from a height of 12.7 cm to a height of 72.4 cm in 11 steps. The sensor output was observed to increase with height. At the equidistant point between the two plates, the field was observed to be 1.27 A/m, or 3 percent higher than calculated.

It was observed that calculating the magnetic field using the SRI[2] formula given below did not agree with the above-measured values or with the calculated value determined from the measured line voltage. Using

$$H = \frac{V_L}{Z_o W}\ , \qquad (1)$$

where

H = magnetic field in amperes/meter ,

V_L = line voltage, in volts (370.0) ,

Z_o = line impedance, in ohms (90.0) ,

and

W = line width, in meters (2.0) ,

yields a value of 2.06 A/m. This is 1.62 times greater than the field determined with the B-dot sensor, and is due to the fringing fields at the edge of the line, causing the effective width of the line to be greater than 2.0 m.

Using a formula (eq A-6) derived in appendix A, we see that the effective width-to-height ratio

$$(W/D)_{eff} = \frac{377}{90} = 4.2\ ,$$

and the physical width-to-height ratio

$$(W/D)_{phy} = \frac{2\ m}{0.8\ m} = 2.5\ .$$

From equation (A-13), the calculated field is 1.68 $\left(\frac{4.2}{2.5}\right)$ times the actual field. This compares with the attained value of 1.62 times the measured field.

2.4 Electric Field Measurements with D-Dot Sensor

The electric field of the transmission line was monitored with an EG&G D-dot sensor (HSD-2A) and was observed to have a value of 452.0 V/m. This is within 3 percent of the B-dot measured and the calculated value.

[1] *Project APACHE RPG/TEMPS Data User Handbook, Appendix D of Test Procedures, Project APACHE EMP Test Series — No. 1, vol. 2, contract DNA 001-78-C-0144 (May 1979).*

[2] *B.C. Tupper et al, EMP Instrumentation Development, Stanford Research Institute, contract DAAK02-69-C-0676 (June 1972). 35, 42, 44, 46.*

3. MAGNETIC FIELD SENSORS

3.1 Sensor Calibration

The short-circuit current for the magnetic field sensor that is mounted on the optical transmitter is

$$I = k_H \ell_{eH} H \ , \qquad (2)$$

where

k_H = enhancement factor ,

ℓ_{eH} = effective length of short-circuited loop ,

and

$\dot{H}$ = field in which sensor/transmitter is immersed .

Since the transfer impedance of the Tektronix CT-2 curent probe is 1 ohm, the above equation can be written

$$V = \left(\frac{1V}{A}\right) k_H \ell_{eH} H \ , \qquad (3)$$

Rewritting equation (3), we have the calibration factor in the form

$$\frac{H}{V} = \frac{1}{k_H \ell_{eH}} \qquad (4)$$

The calibration factors for the H-field sensors were obtained by inserting them in the working-volume mounting ring and coupling their outputs via coaxial cable to an rf shielded oscilloscope. The first measurement of this type used a previously calibrated sensor (SN H102) from the HDL Simulation Branch. The recorded output of this sensor (see fig. 3, p 8) shows a very fast-rising pulse ($t_r < 1$ ns), an aberration, and then an ultimate peak of 26.0 mV, averaged through a sensor inherent ringing. This level of the pulse, used as the sensor's response to the calculated 1.23 A/m magnetic field, gives poor results when one uses the SRI established calibration factor[2] with the enhancement factor removed. The enhancement factor (1.55) was introduced by Vance[3] to account for the field perturbation caused by the cubical metal box on which the sensor is mounted. Removing the enhancement factor, we obtain (0.0464 A/m/mV) (1.55) = 0.0719 A/m/mV, yielding (0.0719 A/m/mV) (26.0 mV) = 1.87 A/m, which is approximately 1.5 times greater than calculated or previously measured. If however, the enhancement factor is not removed, then the field obtained is (0.0464 A/m/mV)(26.0 mV) = 1.21 A/m, which is very close to the calculated value. It was also observed that if the very early time amplitude of the pulse (t = 1 ns) is used, the enhancement factor can be removed with more favorable comparative results, since at t = 1 ns, the peak amplitude is 19.1 mV (including effects of cable loss). We obtain (19.1 mV)(0.0719 A/m/mV) = 1.37 A/m, which is 11 percent greater than calculated.

The response of the H_{III} sensor provided by the HDL Communications Survivability Branch was observed and recorded. Table 1 (p 9) shows the linearity of this class of sensor through the range of magnetic field variation available using this pulse source. Included are columns for amplitude and calibration factors at both 1 and 10 ns in time. Figures 4 and 5 (p 10) show the H-field sensor.

3.2 Sensor Dynamic Range

The dynamic range of this sensor is determined from the maximum and minimum signals, which can be faithfully reproduced. From table 1 the minimum signal which can be observed is approximately 0.45 A/m for a sensor output of 10.0 mV (at t = 10 ns). The maximum signal is determined by the saturation of the Tektronix CT-2 current probe used in this sensor. Calculations indicate that the field levels which could cause saturation are considerably above the levels of interest for EMP experimentation.

---

[2] *B. C. Tupper et al, EMP Instrumentation Development, Stanford Research Institute, contract DAAK02-69-C-0676 (June 1972). 35, 42, 44, 46.*

[3] *E. F. Vance, Field Mapping and Data Analysis for a Long-Wire Antenna (U), Technical Report I, Appendix A, prepared by Stanford Research Institute for U.S. Army Mobility Equipment Research and Development Center (January 1969). (SECRET)*

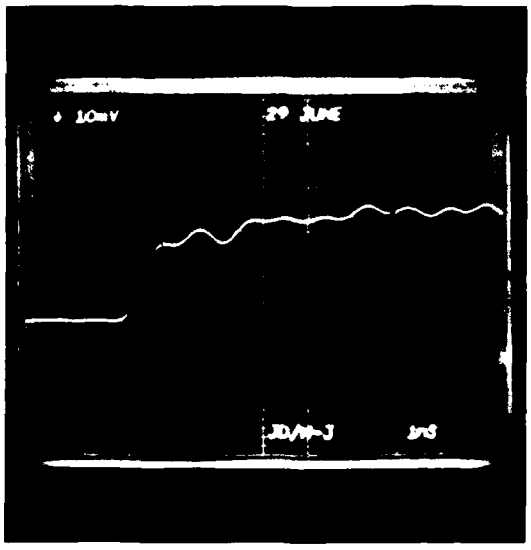

10mv/Div
1ns/Div

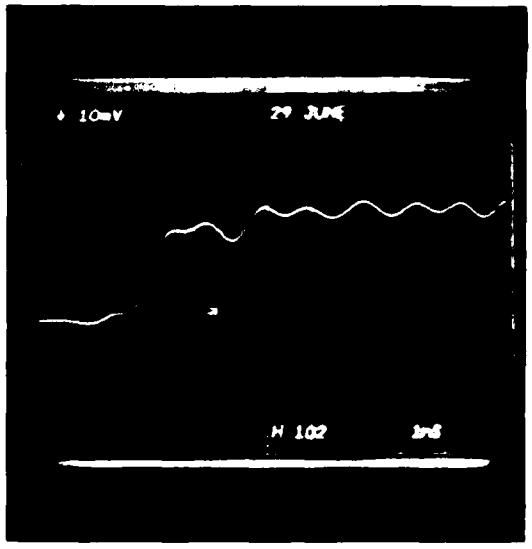

10mv/Div
1ns/Div

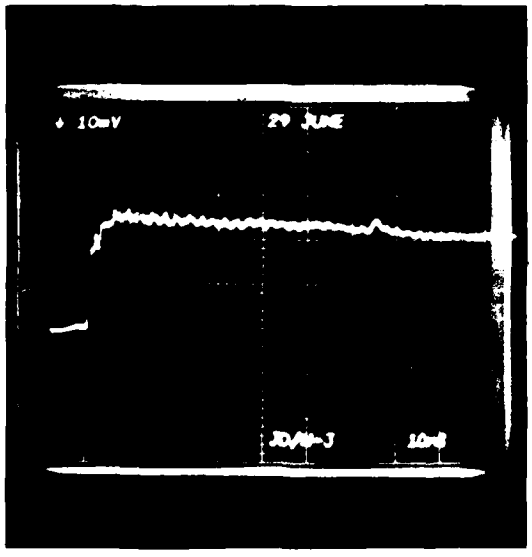

10mv/Div
10ns/Div

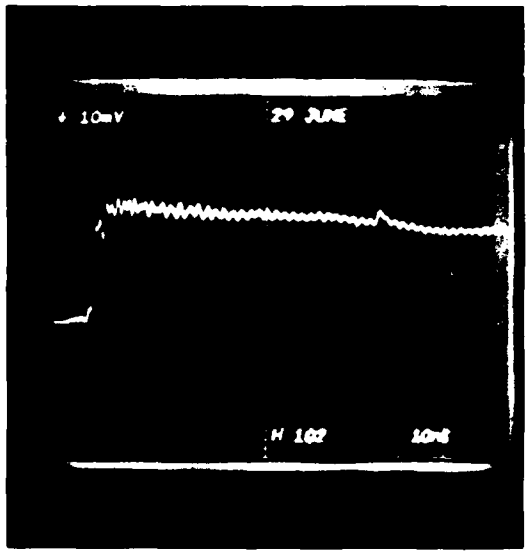

10mv/Div
10ns/Div

Figure 2. Recorded output of H-field sensor, H_{III} (HDL Communications Survivability Branch Sensor).

Figure 3. Recorded output of H-field sensor, H_{III} (HDL Simulation Branch Sensor).

TABLE 1. H_{III} SENSOR OUTPUT VERSUS APPLIED MAGNETIC FIELD

PULSER DIAL (kV)	H-FIELD (A/m)	SENSOR OUT (mV) t = 1 ns	SENSOR OUT (mV) t = 10 ns	A/M/mV 1 ns	A/M/mV 10 ns
0.5	0.308	4.25	6.9	0.0725	0.0447
1.0	0.615	8.5	13.8	0.0725	0.0446
1.5	0.923	12.7	20.7	0.0727	0.0446
2.0	1.23	18.0	26.5	0.0683	0.0464
2.5	1.54	21.2	33.9	0.0726	0.0454
3.0	1.85	24.4	40.3	0.0758	0.0459
				Avg = 0.0724	Avg = 0.0453

3.3 Frequency Response

The high-frequency response of the H-field sensor is estimated from the formula[4] $f_h \simeq 0.35/t_r$, where f_h is the upper 3-dB cutoff frequency and t_r is the time to rise from 10 to 90 percent of the pulse's final value. The result is as follows for the sensor checked.

H_{III} upper 3-dB cutoff frequency $f_h = 140.0$ MHz.*

A small transmission line, designed and constructed for the HDL Scale Model Facility in order to calibrate small sensors, was used to measure the H-field sensor low-frequency response. This 200-cm-long by 8.9-cm-high tapered line (40.6 cm wide) was placed over the sensor mounting ring in the working volume of the transmission line. BNC wall-mount connectors were placed in the lower plate of the line beneath both ends of the small transmission line so that it could be coaxially fed and terminated. A Tektronix 106 pulse generator was used to drive this small line, which was actually 14 cm above the lower plate to accommodate the H-field sensor height.

The H_{III} sensor response to a 5.0 μs square wave pulse was coaxially coupled to the recording instrument. The sensor was found to have an e-fold of 1.8 μs. The low-frequency 3-dB corner for this sensor is calculated to be[2]

$$f = \frac{1}{2\pi\tau_a} = \frac{1}{(6.28)(1.8\times10^{-6})} = 88.5\ \text{kHz},$$

which is in good agreement with the SRI value of 90 kHz.

The H_{III} sensor was then coupled to the recording instrumentation using the fiber-optic transmitter/receiver (channel 2) provided by the HDL Communications Survivability Branch. The H_{III}/channel 2 transmitted data show the low-frequency response to be the same as the direct (coaxially) coupled response of 88.5 kHz (3 dB).

3.4 Enhancement Factor

The H_{III}/channel 2 fiber-optic transmitter (a circular cylinder 14.0 cm high by 11.4 cm diameter) combination was used (as a ground plane sensor) to observe and record the H-field of the large transmission line.

The H_{III}/channel 2 combination was then raised out of the mounting ring so that one-half its

[4] *H. DeWaard and D. Lazarus, Modern Electronics, Addison-Wesley (1966), 155.*

**The H_{III} sensor has a very fast initial risetime, but rounds off near the top of the pulse. The formula does not account for the very fast initial risetime.*

[2] *B. C. Tupper et al, EMP Instrumentation Development, Stanford Research Institute, contract DAAK02-69-C-0674 (June 1972). 35, 42, 44, 46.*

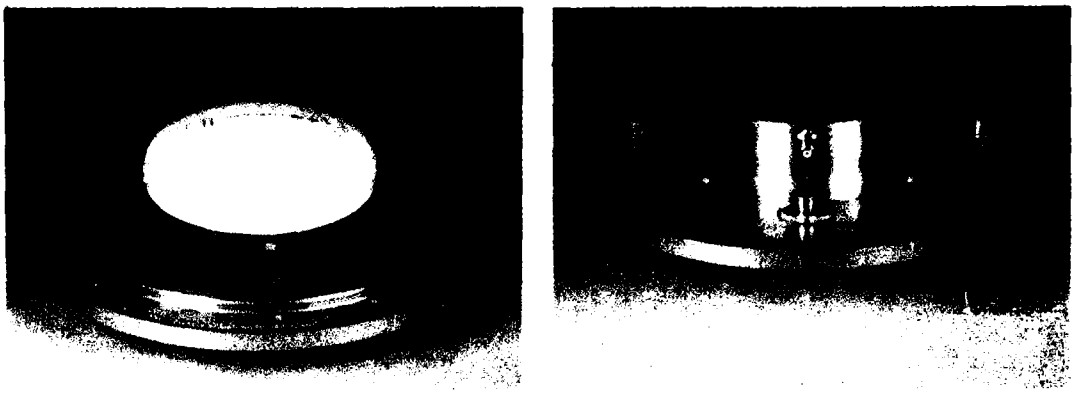

Figure 4. H-field sensor: (a) top and (b) bottom.

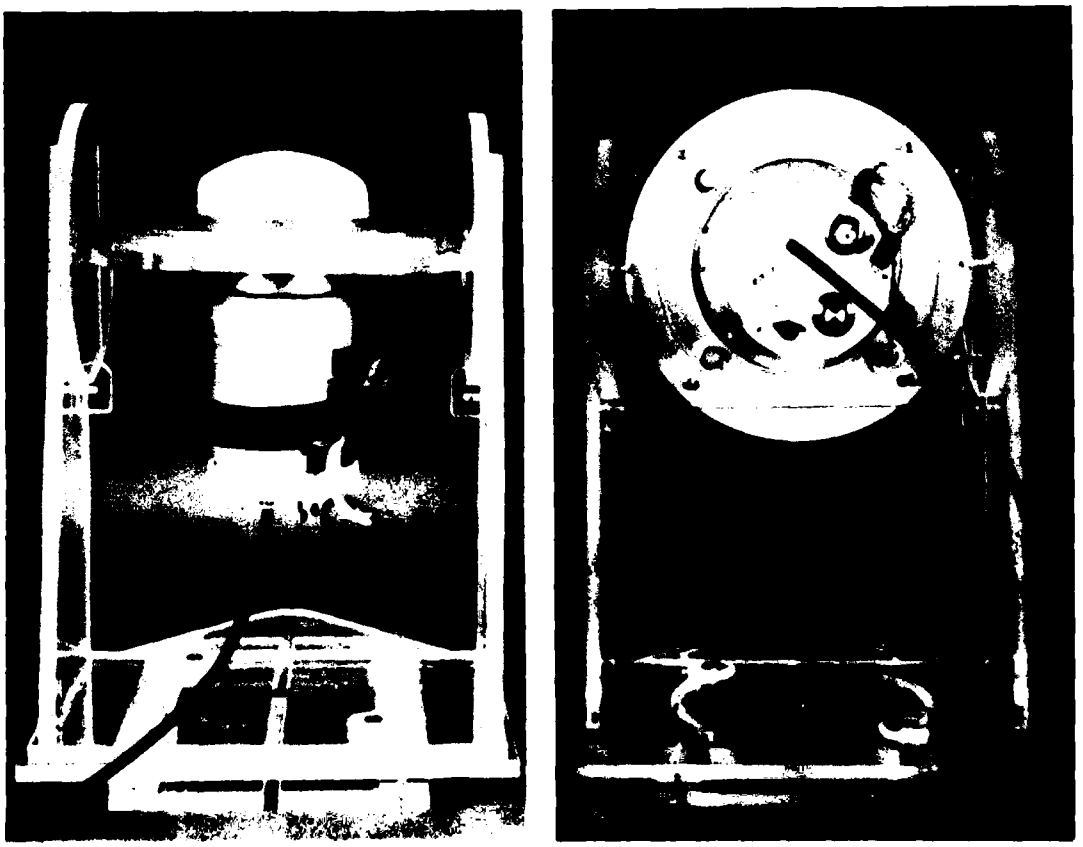

Figure 5. H-field sensor mounted on fiber-optic transmitter: (a) back and (b) side.

length was above the lower plate of the line. Steel wool was inserted between the mounting ring and the fiber-optic transmitter case to maintain contact. The image of the sensor/transmitter was formed by the lower plate, and the incident field effectively illuminated the entire cylindrical structure.[5] This technique was used to eliminate spurious coupling from the sensor/transmitter to the bottom plate.

The results showed no measurable difference in sensor output voltage when the sensor/transmitter was raised. This implies that the enhancement factor, k_H, equals one.

The free-space calibration factor* of the H_{III} sensor/transmitter is then (see table 1),

$$\frac{H}{V} = \frac{0.0453 \text{ A/m/mV}}{1.0} = 0.0453 \text{A/m/mV}.$$

This is an average calibration factor for use at times greater than 10 ns.

4. CONCLUSIONS

The following conclusions can be made from the findings of this report.

a. The use of the SRI-type sensors with an optical system represents a definite improvement in field measurement technology.

b. The SRI calibration factor given in their report[2] for the H_{III} class sensor is for times greater than 10 ns from the zero level of the pulse.

c. The cube-mounted H-field sensor enhancement factor is very close to unity, and the previously attributed value of 1.55 was offset by a calculation error for the magnetic field in the transmission line used to calibrate the original sensors. Appendix A shows that the effective width of the SRI transmission line caused an increase in the magnetic field sensor calibration factor which was cancelled out by the application of the supposed enhancement factor of a cube.

d. An obvious extension of this work is to use the fiber-optic coupled H-field sensor in a free-field environment, comparing its calibrated output with that of other types of sensors.

ACKNOWLEDGEMENTS

The use of the sensors with the fiber-optic system was suggested by Jere Dando, now Chief of the Harry Diamond Laboratories Electronics Branch, previously Chief of the Communications Survivability Branch.

The authors wish to thank William Petty, Chief of the Simulation Branch, for his cooperation in the installation of the transmission line at the Woodbridge Research Facility, as well as for the use of the Simulation Branch's sensors.

The authors also wish to thank Leo Levitt of the Electronics Branch for many interesting discussions relating to the measurement of electromagnetic fields.

---

[2] *B. C. Tupper et al, EMP Instrumentation Development, Stanford Research Institute, contract DAAK02-69-C-0674 (June 1972). 35, 42, 44, 46.*

[5] *R. W. Sassman et al, Electromagnetic Scattering from a Conducting Post, Air Force Weapons Laboratory Sensor and Simulation Notes, Note 45 (June 1967). 45-19.*

* *The use of free-space calibration factor requires the actual sensor output voltage. This is obtained by taking into account the overall fiber-optic system gain.*

Literature Cited

1. *Project APACHE RPG/TEMPS Data User Handbook, Appendix D of Test Procedures, Project APACHE EMP* Test Series, No. 1, Vol. 2, Contract DNA 001-78-C-0144 (May 1979).
2. B. C. Tupper et al, *EMP Instrumentation Development*, Stanford Research Institute, contract DAAK02-69-C-0674 (June 1972), 35, 42, 44, 46.
3. E. F. Vance, *Field Mapping and Data Analysis for a Long-Wire Antenna* (U), Technical Report 1, Appendix A, prepared by Stanford Research Institute, for U.S. Army Mobility Equipment Research and Development Center (January 1969). (SECRET)
4. H. DeWaard and D. Lazarus, *Modern Electronics*, Addison-Wesley (1966), 155.
5. R. W. Sassman et al, *Electromagnetic Scattering from a Conducting Post*, Air Force Weapons Laboratory Sensor and Simulation Notes, Note 45 (June 1967), 45-19.

APPENDIX A. — EFFECT OF ERROR ON CALCULATION OF MAGNETIC FIELD ON SENSOR ENHANCEMENT FACTOR

Here we will attempt to show that the effective width of the Stanford Research Institute (SRI) transmission line caused an increase in the magnetic field sensor calibration factor which was cancelled out by the application of the supposed enhancement factor of a cube.

The original equations used by SRI in their transmission-line field strength calculations are[1]

$$\text{(a)}\quad E = V_L/D\ , \tag{A-1}$$

$$\text{(b)}\quad H = \frac{ED}{Z_o W} = \frac{V_L}{Z_o W}\ , \tag{A-2}$$

where

E = electric field (V/m) ,

H = magnetic field (A/m) ,

V_L = line voltage ,

D = line height* (0.356 m) ,

W = line width (1.83 m) ,

and

Z_o = characteristic line impedance (50 ohms) .

When the formula for the electric field strength and the magnetic field strength are substituted in the formula for the characteristic impedance of free space, the results are as follows.

Since

$$120\pi = E/H \tag{A-3}$$

and

$$120\pi = \frac{V_L/D}{V_L/Z_o W}\ , \tag{A-4}$$

therefore,

$$120\pi = \frac{Z_o W}{D}\ , \tag{A-5}$$

$$377 = Z_o \left(\frac{W}{D}\right) . \tag{A-6}$$

Since the SRI transmission-line impedance (Z_o) was known to be 50 ohms, the effective width-to-height ratio $\left(\frac{W}{D}\right)$ would have to be as follows ($Z_o = 50$).

$$\left(\frac{W}{D}\right)_{eff} = \frac{377}{50}\ , \tag{A-7}$$

$$\left(\frac{W}{D}\right)_{eff} = 7.54\ . \tag{A-8}$$

However, the width-to-height ratio obtained from the physical dimensions of the SRI transmission line is

$$\left(\frac{W}{D}\right)_{phy} = \frac{1.83\ \text{m}}{0.356\ \text{m}} = 5.14\ . \tag{A-9}$$

The larger effective ratio (7.54) can be attributed to the fringing fields at the edge of the SRI line, causing the effective width (now designated as W') of the line to increase. The effect this would have on the magnetic field strength calculation would be the following.

Since, from equation (A-2),

[1] *B. C. Tupper et al, EMP Instrumentation Development, Stanford Research Institute, contract DAAK02-69-C-0674 (June 1972), 43, 44.*

* *SRI used the letter D for line height; this report used h.*

APPENDIX A

$$H = \frac{V_L}{Z_o W}$$

and

$$W' = \frac{7.54}{5.14}\ (W) = 1.47(W)\ , \qquad \text{(A-10)}$$

then

$$H = \frac{V_L}{Z_o \left(\frac{W'}{1.47}\right)} \qquad \text{(A-11)}$$

or

$$H = \frac{1.47\ V_L}{Z_o W'}\ ; \qquad \text{(A-12)}$$

and, finally,

$$H = \frac{(W/D)_{eff}}{(W/D)_{phy}}\ H' = 1.47H'\ , \qquad \text{(A-13)}$$

where H′ equals the actual magnetic field strength and is designated with a prime only in this appendix.

The calculated value of the magnetic field strength would therefore be 1.47 times higher than the actual field strength (H′); hence, the derived ground plane calibration factor [1] would be high by the same factor.

A correction factor ("enhancement factor") was used [1] to account for "field perturbation" caused by the cubical metal box on which the sensor was mounted. It appears that its effect in reality was just to cancel the error caused by the miscalculation of the magnetic field. This we show below. To compute the calibration factor of the sensor when mounted in a ground plane, we use the formula $H/V = 1/l_{eH}$ where l_{eH} is the effective length. However, H is not the correct value, so we must substitute from equation (A-13), yielding

$$\frac{1.47\ H'}{V} = \frac{1}{l_{eH}} \qquad \text{(A-14)}$$

so that

$$\frac{1}{l_{eH}} = \frac{1.47}{l'_{eH}} \qquad \text{(A-15)}$$

where

$$\frac{H'}{V} = \frac{1}{l'_{eH}}$$

and

l'_{eH} = the correct effective length (designated with a prime only in this appendix).

Now, to compute the calibration factor of the sensor when mounted on a metal cube (if we believed H to be correct) we use the formula

$$\frac{H}{V} = \frac{1}{k_H\ l_{eH}}\ ,$$

where $k_H = 1.55$ is the SRI enhancement factor which accounts for the field perturbation of the cube. Substituting from equation (A-15), we obtain

$$\frac{H}{V} = \frac{1.47}{1.55\left(l'_{eH}\right)}\ ,$$

$$\frac{H}{V} = 0.95\left(\frac{1}{l'_{eH}}\right)\ ,$$

which was to be shown.

$$\frac{H}{V} \simeq \frac{1}{l'_{eH}}\ ,$$

where

$\frac{H}{V}$ = calibration factor for the sensor mounted in a ground plane.

[1] *B. C. Tupper et al, EMP Instrumentation Development, Stanford Research Institute, contract DAAK02-69-C-0674 (June 1972), 45.*

DISTRIBUTION

DEFENSE DOCUMENTATION CENTER
CAMERON STATION, BUILDING 5
ATTN DDC-TCA (12 COPIES)
ALEXANDRIA, VA 22314

COMMANDER
USA RSCH & STD GP (EUR)
BOX 65
ATTN LTC JAMES M. KENNEDY, JR.
CHIEF, PHYSICS & MATH BRANCH
FPO NEW YORK 09510

COMMANDER
US ARMY MATERIEL DEVELOPMENT
& READNIESS COMMAND
ATTN DRXAM-TL, HQ TECH LIBRARY
5001 EISENHOWER AVENUE
ALEXANDRIA, VA 22333

COMMANDER
US ARMY ARMAMENT MATERIEL
READINESS COMMAND
ATTN DRSAR-LEP-L, TECHNICAL LIBRARY
ROCK ISLAND, IL 61201

COMMANDER
US ARMY MISSILE & MUNITIONS
CENTER & SCHOOL
ATTN ATSK-CTD-F
REDSTONE ARSENAL, AL 35809

DIRECTOR
US ARMY MATERIEL SYSTEMS
ANALYSIS ACTIVITY
ATTN DRXSY-MP
ABERDEEN PROVING GROUND, MD 21005

DIRECTOR
US ARMY BALLISTIC RESEARCH LABORATORY
ATTN DRDAR-TSB-S (STINFO)
ABERDEEN PROVING GROUND, MD 21005

TELEDYNE BROWN ENGINEERING
CUMMINGS RESEARCH PARK
ATTN DR. MELVIN L. PRICE, MS-44
HUNTSVILLE, AL 35807

ENGINEERING SOCIETIES LIBRARY
345 EAST 47TH STREET
ATTN ACQUISITIONS DEPARTMENT
NEW YORK, NY 10017

US ARMY ELECTRONICS TECHNOLOGY
& DEVICES LABORATORY
ATTN DELET-DD
FORT MONMOUTH, NJ 07703

DIRECTOR
DEFENSE ADVANCED RESEARCH
PROJECTS AGENCY
ATCHITECT BLDG
ATTN DIR, NUCLEAR MONITORING RES OFFICE
1400 WILSON BLVD
ARLINGTON, VA 22209

DEFENSE COMMUNICATION
ENGINEERING CENTER
ATTN TECHNICAL LIBRARY
1860 WIEHLE AVE
RESTON, VA 22090

DIRECTOR
DEFENSE COMMUNICATIONS AGENCY
DEPT OF DEFENSE
ATTN TECH LIBRARY
WASHINGTON, DC 20305

DIRECTOR
DEFENSE COMMUNICATIONS AGENCY
COMMAND & CONTROL TECHNICAL CENTER
ATTN TECHNICAL DIRECTOR (C300)
WASHINGTON, DC 20301

DIRECTOR
DEFENSE NUCLEAR AGENCY
ATTN ELECTRONIC VULNERABILITY DIV (RAEV)
ATTN TECHNICAL LIBRARY (TITL)
ATTN INFORMATION SYSTEMS DIV (VLIS)
WASHINGTON, DC 20305

UNDER SECRETARY OF DEFENSE
FOR RESEARCH & ENGINEERING
ATTN ASST DIR (ELECTRONICS &
PHYSICAL SCIENCES)
ATTN ASST DIR (ENG TECHNOLOGY)
ATTN DEP DIR (STRATEGIC & SPACE SYS)
WASHINGTON, DC 20301

COMMANDER
FIELD COMMAND
DEFENSE NUCLEAR AGENCY
ATTN FCSD-A4, TECH REF BR
KIRTLAND AFB, NM 87115

DIRECTOR
NATIONAL SECURITY AGENCY
ATTN TECHNICAL LIBRARY
FORT GEORGE G. MEADE, MD 20755

OFFICE, DEPUTY CHIEF OF STAFF FOR
OPERATIONS & PLANS
DEPT OF THE ARMY
ATTN DAMO-SSA, NUCLEAR/CHEMICAL
PLANS & POLICY DIV
WASHINGTON, DC 20310

DISTRIBUTION (Cont'd)

COMMANDER
BALLISTIC MISSILE DEFENSE SYSTEMS COMMAND
ATTN TECH LIB
PO BOX 1500
HUNTSVILLE, AL 35807

COMMANDER
BALLISTIC MISSILE DEFENSE ADVANCED
TECHNOLOGY CENTER
ATTN TECH LIB
PO BOX 1500
HUNTSVILLE, AL 35807

COMMANDER
US ARMY COMMUNICATIONS COMMAND
ATTN TECH LIB
FORT HUACHUCA, AZ 85613

CHIEF
US ARMY COMMUNICATIONS SYS AGENCY
ATTN SCCM-AD-SV, LIBRARY
FORT MONMOUTH, NJ 07703

COMMANDER
US ARMY NUCLEAR & CHEMICAL AGENCY
BUILDING 2073
ATTN TECH LIB
7500 BACKLICK ROAD
SPRINGFIELD, VA 22150

COMMANDER
CORPS OF ENGINEERS
HUNTSVILLE DIVISION
ATTN T. BOLT
PO BOX 1600
HUNTSVILLE, AL 35807

COMMANDER
NAVAL SURFACE WEAPONS CENTER
ATTN WA-50, NUCLEAR WEAPONS
EFFECTS DIV
WHITE OAK, MD 20910

COMMANDER
AF WEAPONS LAB, AFSC
ATTN SE, NUCLEAR SYS DIV
ATTN EL, ELECTRONICS DIV
KIRTLAND AFB, NM 87117

UNIVERSITY OF CALIFORNIA
LAWRENCE LIVERMORE LABORATORY
ATTN E. K. MILLER
PO BOX 808
LIVERMORE, CA 94550

ITT RESEARCH INSTITUTE
ATTN I. N. MINDEL
ATTN J. E. BRIDGES
10 WEST 35TH STREET
CHICAGO, IL 60616

KAMAN SCIENCES CORP
PO BOX 7463
COLORADO SPRINGS, CO 80933

STANFORD RESEARCH INSTITUTE
ATTN A. L. WHITSON
ATTN E. VANCE
3980 EL CAMINO REAL
PALO ALTO, CA 94306

US ARMY ELECTRONICS RESEARCH
& DEVELOPMENT COMMAND
ATTN TECHNICAL DIRECTOR, DRDEL-CT

HARRY DIAMOND LABORATORIES
ATTN 00100, COMMANDER/TECH DIR/TSO
ATTN CHIEF, DIV 10000
ATTN CHIEF, DIV 20000
ATTN CHIEF, DIV 30000
ATTN CHIEF, DIV 40000
ATTN RECORD COPY, 81200
ATTN HDL LIBRARY, 81100 (3 COPIES)
ATTN HDL LIBRARY, 81100 (WOODBRIDGE)
ATTN TECHNICAL REPORTS BRANCH, 81300
ATTN CHAIRMAN, EDITORIAL COMMITTEE
ATTN CHIEF, 21000
ATTN CHIEF, 21100
ATTN CHIEF, 21200
ATTN CHIEF, 21300
ATTN CHIEF, 21400
ATTN CHIEF, 21500
ATTN CHIEF, 22000
ATTN CHIEF, 22100
ATTN CHIEF, 22300
ATTN CHIEF, 22800
ATTN CHIEF, 22900
ATTN SPOHN, D., 21300
ATTN LANHAM, C., 00210
ATTN WIMENITZ, F., 20240
ATTN CLARK, S., 21100
ATTN WASHINGTON, J., 21100
ATTN LOFTUS, J. J., 21400
ATTN CUNEO, A. A., 21400 (30 COPIES)